IX. COMMUNICATIONS RESEARCH

A. MULTIPATH TRANSMISSION

Prof. L. B. Arguimbau   J. Granlund
E. H. Gibbons, Jr.   W. L. Hatton

1. Speech and Music

During the past quarterly period, an expression was derived heuristically which gives the root-mean-square interference resulting from the multipath transmission of frequency-modulated signals. The expression also holds for the important case of common-channel interference between two stations. Experimental checks show that the operation of our laboratory receiver agrees fairly well with the formula for an ideal receiver, provided the desired signal exceeds the undesired by a half decibel.

For a ratio a of undesired signal to desired signal, and an instantaneous difference frequency, ν, the interference may be expressed as:

$$\Delta f_o = - \frac{\nu a}{1 + a^2} \; \frac{a + \cos 2\pi\nu t}{1 + \left[\frac{2a}{1 + a^2}\right] \cos 2\pi\nu t} \quad , \qquad o \leqslant a \leqslant 1 , \tag{1}$$

which may be expanded to

$$\Delta f_o = \nu \sum_{n=1} (-a)^n \cos 2\pi n\nu t \quad . \tag{2}$$

The instantaneous power associated with this interference is proportional to

$$\overline{\Delta f_o}^2 = \frac{1}{2} \nu^2 \sum_{n=1} a^{2n} = \frac{1}{2}\left(\frac{\nu^2}{1 - a^2}\right) \quad . \tag{3}$$

The deemphasis circuit and an appropriate low-pass filter have the characteristics

$$\left| Z_{12} \right|^2 = \frac{1}{1 + \left[2\pi(75 \times 10^{-6})\ \nu\right]^2}$$

and (4)

$$\left| Z_{12} \right|^2 = \frac{1}{1 + \left[\frac{\nu}{13 \times 10^3}\right]^6}$$

respectively. After the interference has been filtered by these, the instantaneous power associated with the difference frequency, ν , varies as

$$\overline{\Delta f_1(\nu,a)}^2 =$$

$$\frac{1}{2}\,\nu^2 \sum_{n=1} a^{2n} \frac{1}{1+\left[2\pi(75\times 10^{-6})n\nu\right]^2}\;\frac{1}{1+\left[\dfrac{n\nu}{13\times 10^3}\right]^6} \quad . \tag{5}$$

This instantaneous power after filtering has been computed as a function of the instantaneous difference frequency, ν, for various signal-amplitude ratios, $\underline{a}$.

The interference power is computed above on the assumption that the two signals have a constant frequency difference. We are actually interested in knowing the interference when the frequency difference varies sinusoidally. In all of the work, we have held to the concept of a variable instantaneous frequency rather than to a spectrum respresentation. Here it seems logical to permit the instantaneous frequency difference between the two signals to vary sinusoidally and to think of the root-mean-square interference as varying accordingly. If the frequency variation is slow enough, it seems quite definite that the total interference is merely the time average of the varying interference. How far this method is appropriate, whether or not it can be used for audio-frequency variations, is less clear. It is hoped that justification can be made for the following calculations which are based on such an assumption.

When the difference frequency varies sinusoidally according to

$$\nu = \nu_m \sin\theta \tag{6}$$

the average interference power is proportional to

$$\overline{\Delta f_2(\nu_m,a)}^2 = \frac{2}{\pi}\int_0^{\pi/2} \overline{\Delta f_1(\nu_m \sin\theta,\ a)}^2 \quad d\theta \quad . \tag{7}$$

The function

$$\Delta f = \sqrt{\frac{4}{\pi}\int_0^{\pi/2} \overline{\Delta f_1(\nu_m \sin\theta,\ a)}^2 \quad d\theta} \tag{8}$$

is plotted in Figure IX-1. against the peak difference frequency, ν_m, for various amplitude ratios, $\underline{a}$. It will be observed that Δf is the peak value of the sinusoid which would give the same interference power as the actual filtered interference. The indicated integration was carried out by the joint computing group.

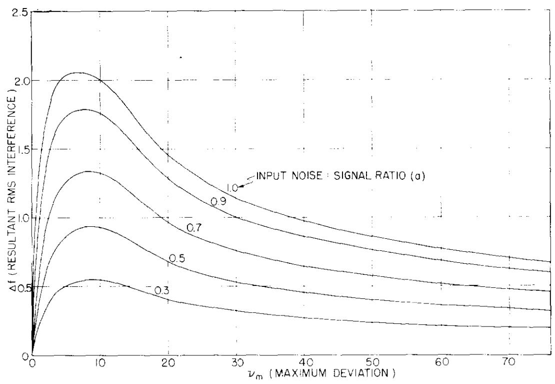

Fig. IX-1 Resultant rms interference vs. peak difference frequency for various amplitude ratios.

Concurrently with the interference calculations and measurements, a tuner for the field-test receiver was constructed and aligned. The r-f section consists of a single amplifier. The grid circuit is an overcoupled transformer designed for approximately optimum noise figure, while the plate circuit is single-tuned with an adjustable Q. The overall transfer characteristic is Butterworth with n = 3, and has a bandwidth of 400 kc. This characteristic is flat within 1 per cent over a 200-kc range, as required by the condition that the roles of "stronger" and "weaker" signal shall not interchange during an audio cycle.

Prof. L. B. Arguimbau, E. H. Gibbons, Jr., J. Granlund

2. Television

The system for displaying the effects of two-path transmission on AM television has been set up, and the expected "ghosts" observed. The experimental setup is shown in block form in Figure IX-2.

The combined camera and synchronizing generator is part of a television system intended for use in directing guided bombs. It is used in conjunction with a slide projector which throws the image of a standard R. M. A. resolution chart directly on the mosaic of the iconoscope tube. The line and frame characteristics are non-standard, there being a total of 330 lines in a frame at 40 frames per second. There is no interlace. The quality is not equivalent to that of commercial standards, but it is felt that it is sufficient for the present purposes.

The square-wave generator delivers square waves with repetition rates of 80 to 200 kc/sec or pulses of about half-microsecond duration and from 3-to 60-microsecond repetition period. Since the available rise time is of the order of 0.01 microsecond it is also used to test the other components in the system.

The transmitter section triples three times from a 7.4074-Mc crystal

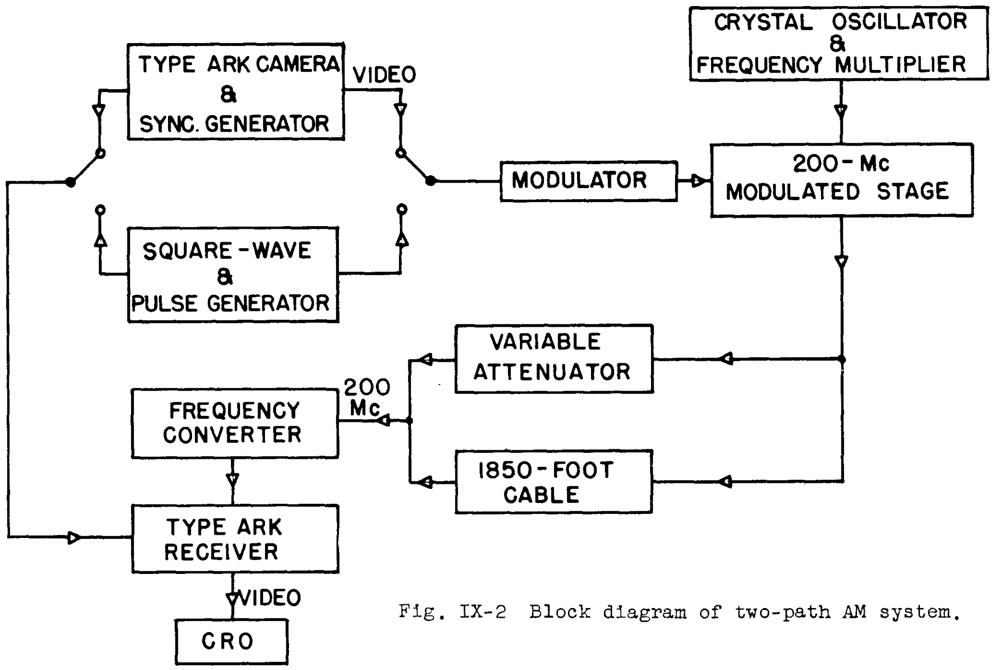

Fig. IX-2 Block diagram of two-path AM system.

oscillator to drive the 200-Mc grid-modulated final. The final delivers about 3/4 watt to the two paths in parallel.

The signals from the two paths are added and applied to the input of the frequency converter. The output of the converter is at 50 Mc/sec so that the existing Δif strip in the receiver can be used.

The receiver was formerly part of the same bombing system as the transmitter, and has comparable quality. A cathode-ray oscilloscope is connected to the receiver video circuits so that the waveform can be observed in addition to the picture-tube display.

The receiver is synchronized separately, therefore the effect of the two-path transmission on the synchronizing has not been studied. This phase of the project may be taken up after the FM system has been completed. The separate synchronizing circuit has the advantage of giving clearer picture-tube displays.

The two-path transmission effects can be studied with any of the three waveforms available:

1. The square-wave generator is set so that the repetition period is longer than twice the delay of the cable. The resulting waveforms and picture-tube display are shown in Figure IX-3.

2. The pulse output from the generator is set so that the pulse width is shorter than the cable delay, while the repetition

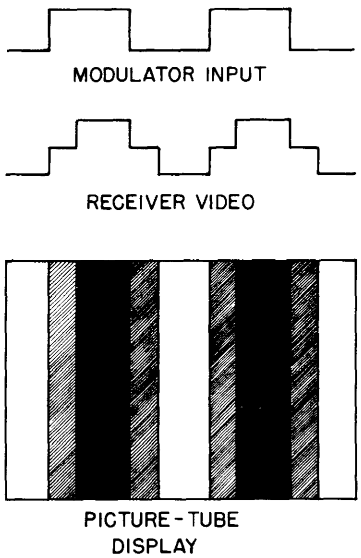

Fig. IX-3 Square-wave response in two-path system with equal signal strength on each path.

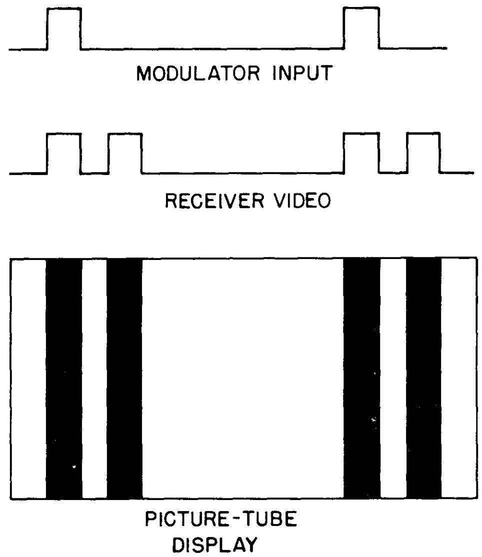

Fig. IX-4 Pulse response in two-path system with equal signal strength on each path.

period is longer. Resulting waveforms are shown in Figure IX-4.

3. The camera is used to transmit the resolution chart. The waveforms are too complex to be drawn, but the effect on the picture-tube display is similar to that seen on standard receivers under multipath conditions. In the experimental system, however, there is only one "ghost".

Now that we have produced a laboratory system for simulating the multipath transmission occuring in practice, it remains to construct an FM system and to check its operation against the AM system.

W. L. Hatton

B. MICROWAVE MODULATION TECHNIQUES

L. D. Smullin
J. Jensen
W. E. Vivian

1. Double-Tuned Oscillators

The admittance characteristics of certain multiply excited, externally modulated, nonlinear elements have been investigated. Heterodyne modulation of a double-tuned oscillator (see Figure IX-5) has been observed to create a voltage spectrum containing, as a rule, only a few voltages of appreciable magnitude. Since the frequency differences in this spectrum are observed to be commensurate with the modulation frequencies impressed (see Figure IX-6), one can readily approximate the excitation spectrum and hence find the type of admittance variation occuring in the oscillator.

For example (power series approach):

Assume: $v = V_1 \sin(\omega_1 t) + V_2 \sin(\omega_2 t + \varphi_2)$;

Approximate: $i = a_1 v + a_2 v^2 + a_3 v^3$;

Modulate: $a_1 = a_{10} + a_{11} \sin(\omega_m t + \varphi_{11})$;

Lock Spectrum: $\omega_2 = \omega_1 - \omega_m;\ \omega_m \ll \omega_1$.

Then:

$$Y(V_1,\omega_1) = a_{10} + \tfrac{3}{4}a_{30}(V_1^2 + 2V_2^2) + \tfrac{1}{2}a_{11}\ \frac{V_2}{V_1}\ \angle\psi$$

$$Y(V_2,\omega_2) = a_{10} + \tfrac{3}{4}a_{30}(V_2^2 + 2V_1^2) + \tfrac{1}{2}a_{11}\ \frac{V_2}{V_1}\ \angle{-\psi}$$

where: $\psi = \varphi_2 + \varphi_{11} - \frac{\pi}{2}$

Thus for such a voltage spectrum (one which is often met experimentally) the admittances are:

(1) symmetric in V_1, V_2,
(2) contain real, amplitude-damped terms (a_{10} 0 a_{30}),
(3) contain reactive terms, the amplitudes inversely related, the phases of equal value but opposite sign.

For steady-state oscillation, the sum of the electronic and circuit admittances at each frequency must be zero; hence one can determine the possible modes of oscillation and the effect of modulation on the oscillator by finding the values of V,ω etc., satisfying this condition.

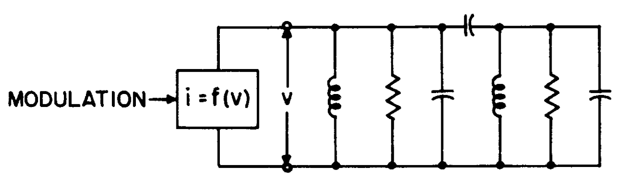

Fig. IX-5 Typical oscillator circuit.

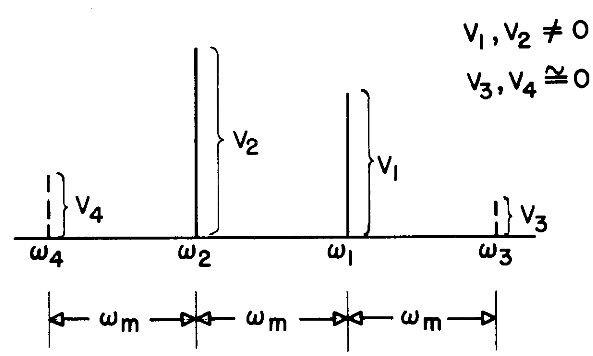

Fig. IX-6 Oscillator spectrum.

Using the expressions derived for the electronic admittances, a number of calculations of modulated oscillator spectra have been made. The computed behaviors check well with experimental observations made on a transitron oscillator at 200 kc.

Some buildup curves for oscillators have been run off on the Macnee differential analyzer. These show mode power versus time for the two frequencies excited when an unmodulated double-tuned oscillator is switched on. The analyzer can also be used to determine the transitional conditions at which a shift in mode will occur.

An effort has been made to find the admittance functions of a reflector-modulated reflex-klystron oscillator, following the same approach as indicated above. Experimental confirmation of the validity of certain approximations appears necessary before any weight can be given to the derived equations.

2. Investigation of Frequency Modulation of a Reflex Klystron

A study is being made of the distortion and power output of a frequency-modulated reflex klystron. A 30-Mc subcarrier is applied to the repeller grid of an S-band klystron. The first sideband of the resulting frequency-modulated wave is extracted and the primary modulation recovered.

In order to make the first-sideband power as large as possible the klystron is modulated over a large part of the mode. Considerable harmonic distortion would therefore be expected if the subcarrier is amplitude-modulated. The distortion can be computed analytically, assuming idealized characteristic curves of frequency and power output versus repeller voltage, as shown in Figure IX-7 below.

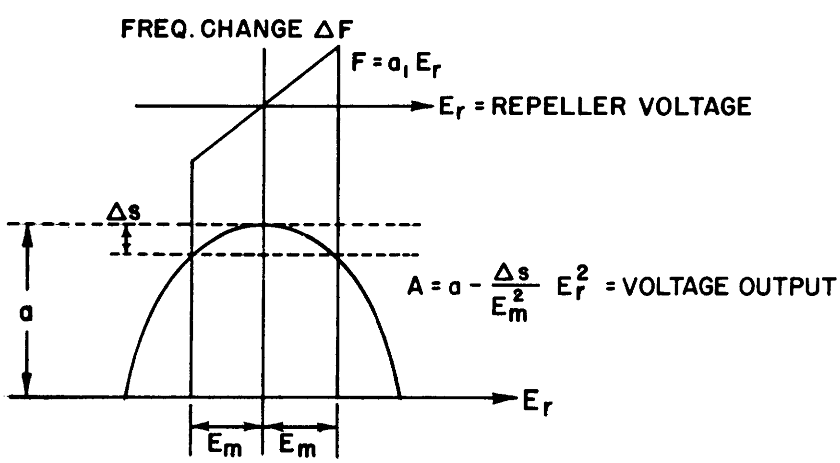

Fig.IX-7 Idealized klystron characteristics.

The expression for the output spectrum about the first sideband does, however, become so unwieldy as to make it useless for practical computation. From a knowledge of the frequency spectrum, the actual distortion can be computed by a rather lengthy process (1).

The actual characteristics of the 726C klystron under investigation deviate so much from the ideal ones mentioned above that no effort has been made to go through numerical computations for the purpose of comparing calculated and observed values.

No analytical expression has been derived for the distortion when the subcarrier is frequency-modulated. At the present moment, some auxiliary equipment is being constructed in preparation for direct distortion measurements.

3. Magnetron Reactance Tube

Work on this project has been summarized in Technical Report No. 94.

C. STATISTICAL THEORY OF COMMUNICATION

Prof. R. M. Fano	N. H. Knudtzon
Prof. Y. W. Lee	E. R. Kretzmer
Prof. J. B. Wiesner	A. J. Lephakis
T. P. Cheatham, Jr.	L. Levine
W. B. Davenport, Jr.	H. E. Singleton
E. E. David, Jr.	B. Steinberg
L. Dolansky	C. A. Stutt

1. Auto-Correlation Function

a. Correlation Functions

The application of the electronic correlator to the problem of detecting a pure tone in random noise has been used to illustrate one of the simplest and more important properties of correlation functions. It can be shown that theoretically the properties of auto-correlation alone will give infinite detectability for an arbitrarily small periodic signal component located in any random time function. "Theoretically", however, requires an infinite period of correlation, and evaluation and measurement of the practical case where this period is finite has been made.

In order to arrive at a rough idea of the notions involved, let $f_1(t)$ be a time function consisting of a periodic signal plus random noise. The auto-correlation function of $f_1(t)$ will be made up of four terms; one term will be the auto-correlation of the signal component -- it will be non-zero; two terms will be cross-correlations of signal and noise components -- these will be identically zero; and the fourth term will be the auto-correlation of the noise component. This term will be zero for large τ, and can be made zero for all τ by compensation. The first term is the desired signal and the last three are, essentially, noise terms whose dispersion approaches zero as a function of the number of samples computed by the correlator. It is important to note that there are at least three effective noise terms and, actually, a fourth if we include a certain amount of dispersion in measuring the signal term in a finite length of time.

It is clear that a practical use of the properties of auto-correlation would be in the detection of a periodic signal in random noise where the only a priori knowledge of the signal is its probable location within a certain bandwidth. However, from the notions of information theory, we know that if, presumptively, any of the three constants (phase angle, amplitude, or frequency) of a sinusoid under detection are known, this information should be of some advantage in the detection of the sinusoid. A practical demonstration of this notion is that, with a knowledge of the frequency of the signal it is desired to detect, one can locally generate as an input to the second channel of the correlator a sinusoid of the same frequency -- thus measuring cross-correlation. In this case, it will be found that the cross-correlation $\varphi_{12}(\tau)$ will be made up of the desired-signal component and only one effective noise term. Cross-correlation has, therefore, reduced the effective number of noise terms from three to one, or, if the effect of a dispersion in the measurement of the signal component is included, from four to two.

It is important to note that since no a priori knowledge of the phase-angle constant has been assumed, the maximum of the signal cross-correlation component must be determined. This will require a measurement of the correlation curve at a minimum of two different valves of τ. However, if it is assumed that, a priori, both the frequency and phase of the desired signal are known, then there will be no ambiguity as to the position of the maximum, since it must occur at $\tau = 0$, T, 2T, etc., where T is the period of the sinusoid. It can be shown that the advantage of knowing the frequency constant of a sinusoid will be a logarithmic function of the input signal-to-noise ratio, whereas additional a priori knowledge of the phase constant will give only a constant 3 db improvement, independent of the input signal-to-noise ratio.

In Figure IX-8 the signal-to-noise ratio at the output of the correlator

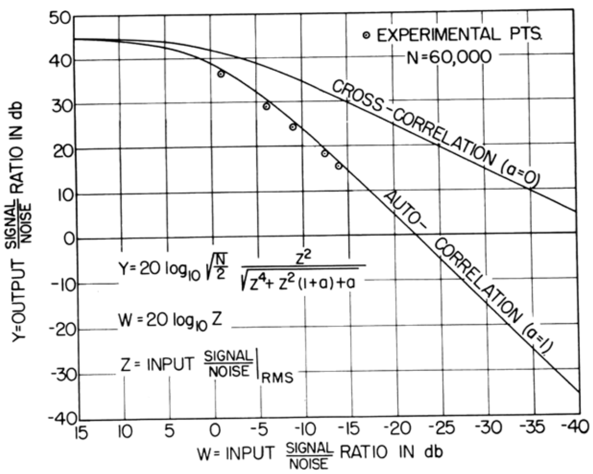

Fig IX-8 Improvement in signal-to-noise ratio through auto-correlation and cross-correlation.

in db has been plotted as a function of the input signal-to-noise ratio in db for N, the number of samples = 60,000. The parameter a in the equation for y is introduced to show the transition from auto- to cross-correlation; a = 1 for auto-correlation and a = 0 for cross-correlation. The difference between these two curves is the advantage to be gained from cross-correlation over auto-correlation as a result of an a priori knowledge of frequency. This difference is plotted in Figure IX-9, and it should be noted that the curve is independent of N, the number of samples. As an example, if a certain output signal-to-noise ratio in db could have been obtained through auto-correlation for an input signal-to-noise ratio of, say, -40 db, then a possibility of switching to cross-correlation through a knowledge of the frequency constant will give a +40 db improvement. As a point of some interest, it can be shown that an attempt to use cross-correlation in the

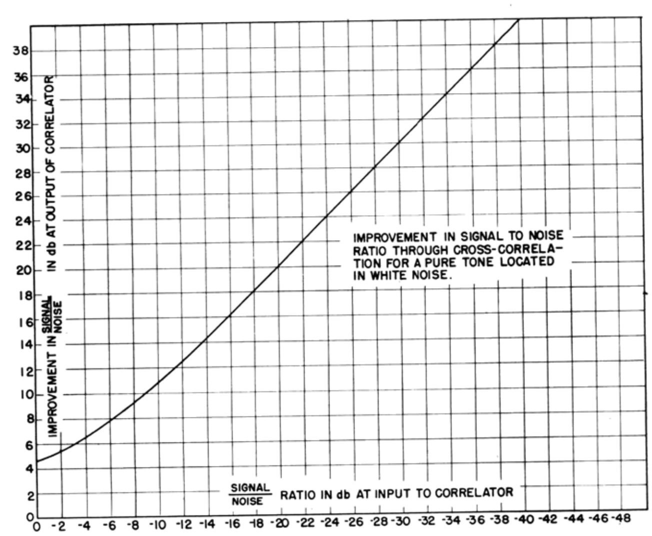

Fig. IX-9 Improvement in signal-to-noise ratio through cross-correlation for a pure tone located in white noise.

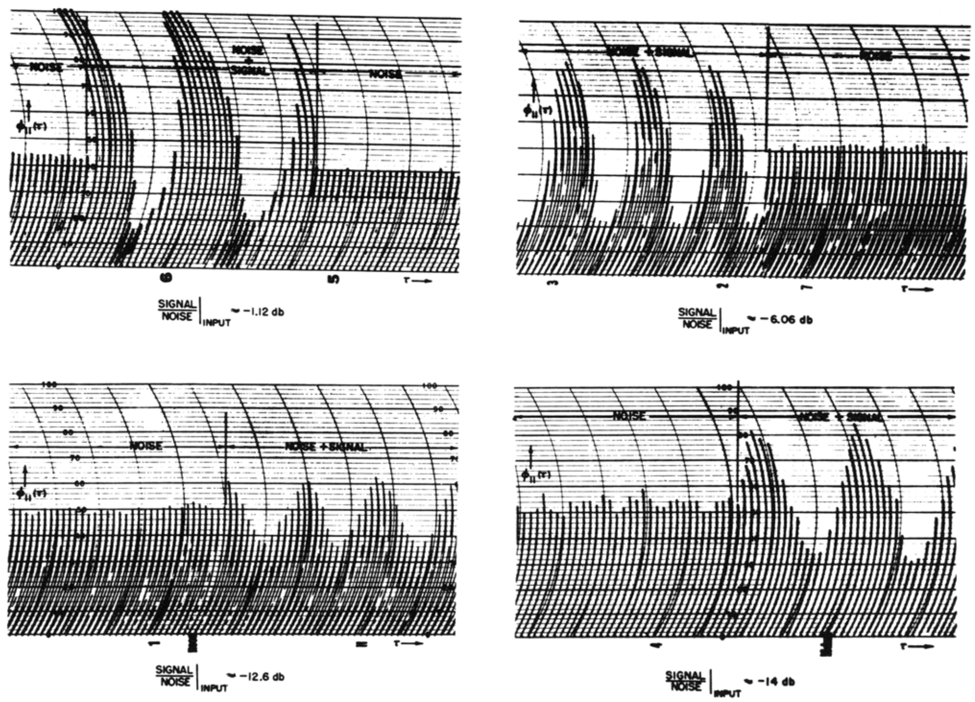

Fig. IX-10 Experimental results showing use of auto-correlation in the detection of a pure tone (8 kc sine wave) in random noise.

detection of a signal of unknown frequency by "hunting" will give no advantage over auto-correlation.

Experimental measurements which check the above results for the case of auto-correlation are shown in Figure IX-10. As a quantitative illustration, the graph in the lower right hand corner of Figure IX-10, for an input signal-to-noise ratio of -14 db, would correspond, in the frequency domain, to a reduction in bandwidth about the desired signal to 0.1 per cent.

Prof. J. B. Wiesner, Prof. Y. W. Lee, T. P. Cheatham, Jr.

b. <u>Auto-correlation Functions of Random Noise</u>

The distribution function and density for the envelope and the zero-crossing frequency for the instantaneous voltage have been investigated for random noise through different filters. Several laboratory amplifiers and a gas tube 884 were used as noise sources. Inasmuch as these results will be published shortly in a Technical Report, only one example is included here. Figure IX-11 shows the normalized envelope distribution density for noise from 884 after a single-tuned circuit with Q = 14 and resonant frequency 20 kc/sec. As will be seen, the experimental points follow the

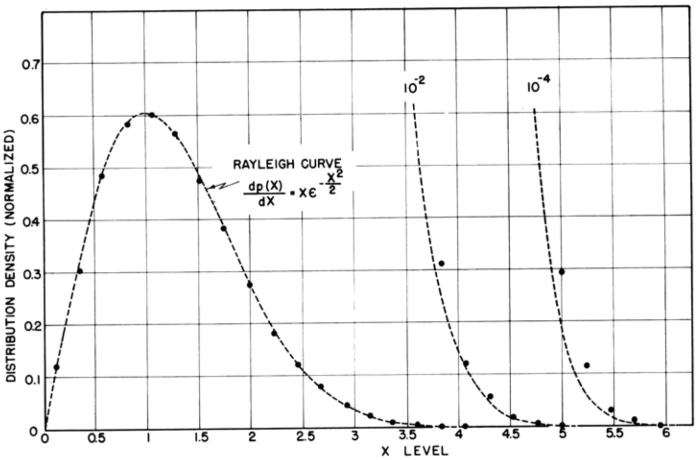

Fig IX-11 Measured and calculated distribution density of random noise filtered by a single-tuned circuit.

theoretical Rayleigh curve quite closely. It may be mentioned that during an observation time of five hours, 8 noise peaks exceeded a level equal to 6.3 times the rms value of the noise.

Similar investigations are now being made for an Eimac 15E operated under space-charge and temperature-limited conditions.

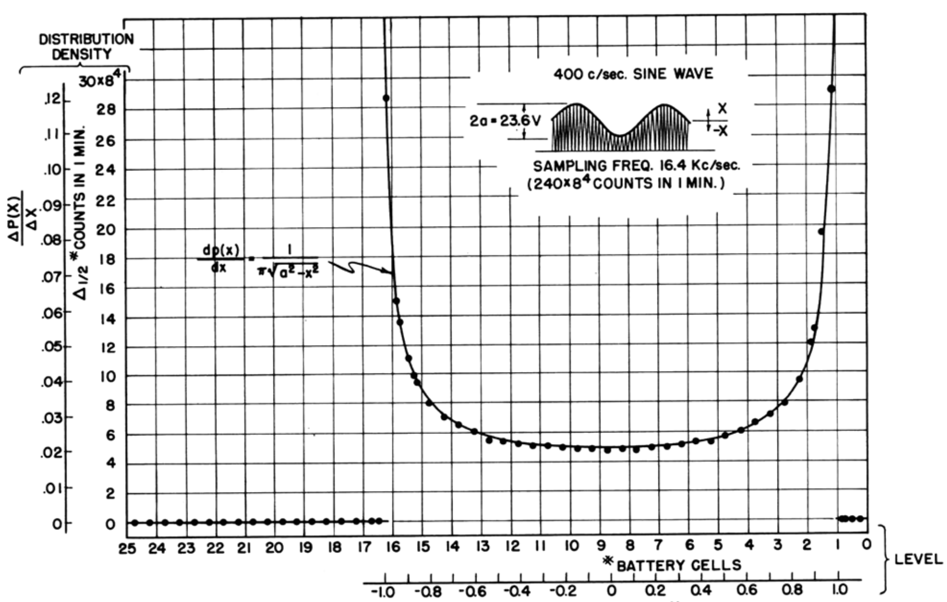

Fig. IX-12 Measured and calculated distribution density of a sine wave.

In order to check the Distribution Analyzer, an AM wave of 16.4 kc/sec, modulated with 400 c/sec, was measured in the same way as the noise. The result is shown in Figure IX-12 where the points are determined by experiment, and the curve is the theoretical distribution density for a sine wave.

Prof. J. B. Wiesner, Prof. Y. W. Lee, N. H. Knudtzon

c. Digital Electronic Correlator

Construction of the digital electronic correlator is about two-thirds completed, and the remaining parts are in the shop. Without auxiliary equipment, the correlator is intended to handle signals with frequency components varying from 10 cps to 10^7 cps -- a dynamic frequency range of 10^6. This range is adequate for radar and television signals.

For signals having lower frequency components -- down to about 1/10 cps -- we propose to use the storage system described elsewhere in this report (see Sec. IX-5). This will allow 100 ten-digit binary numbers to be stored, and will increase the speed of the correlator by a factor of 100.

For signals having frequency components substantially lower than 1/10 cps, as in some servo-mechanisms, we expect to use magnetic tape as a storage medium. This will decrease the dynamic frequency range from 10^6 to 10^4, but this latter range is adequate for most problems. Here, two methods are being worked out. In one method, the continuous input data are to be converted to binary digits in the correlator's coding circuits and the binary digits are to be recorded on the magnetic tape. A pickup head spaced along the tape from the recording head will then give the long delays required.

In the other method of correlating very-low-frequency signals, the continuous signal is to be recorded directly on the magnetic tape while the tape is moving at very slow speed -- say 0.01 inch/sec, in the case of a signal ranging from 10^{-3} cps to 10 cps. A hundred hours of recording will use about 300 feet of tape, and should give an adequate sample. By removing the data from the tape with the tape running at normal speed (about 10 inches/sec) the frequencies will be multiplied by 1000, giving a new range extending from 1 cps to 10^4 cps. The frequency response of this system can easily be made flat over this range by means of suitable equalization. Using this method of multiplying the frequencies will, in combination with the storage system mentioned above, allow the complete correlation function of a low-frequency signal to be obtained in less than an hour.

Prof. Y. W. Lee, H. E. Singleton, T. P. Cheatham, Jr.

2. Amplitude and Conditional Probability Distributions of a Quantized Time Function

The construction and calibration of the amplitude and conditional-probability analyzers discussed in previous progress reports has been completed. In order to obtain an accuracy check, this equipment is being used to determine experimentally the probability distributions of sine waves.

A conditional-probability analyzer is being designed for the study of the zero-crossing periods of the voice. A block diagram of this analyzer is shown in Figure IX-13(a). The conditional probability of interest is the probability of occurrence, as a function of period length, of the nth period after any period having an a priori specified length.

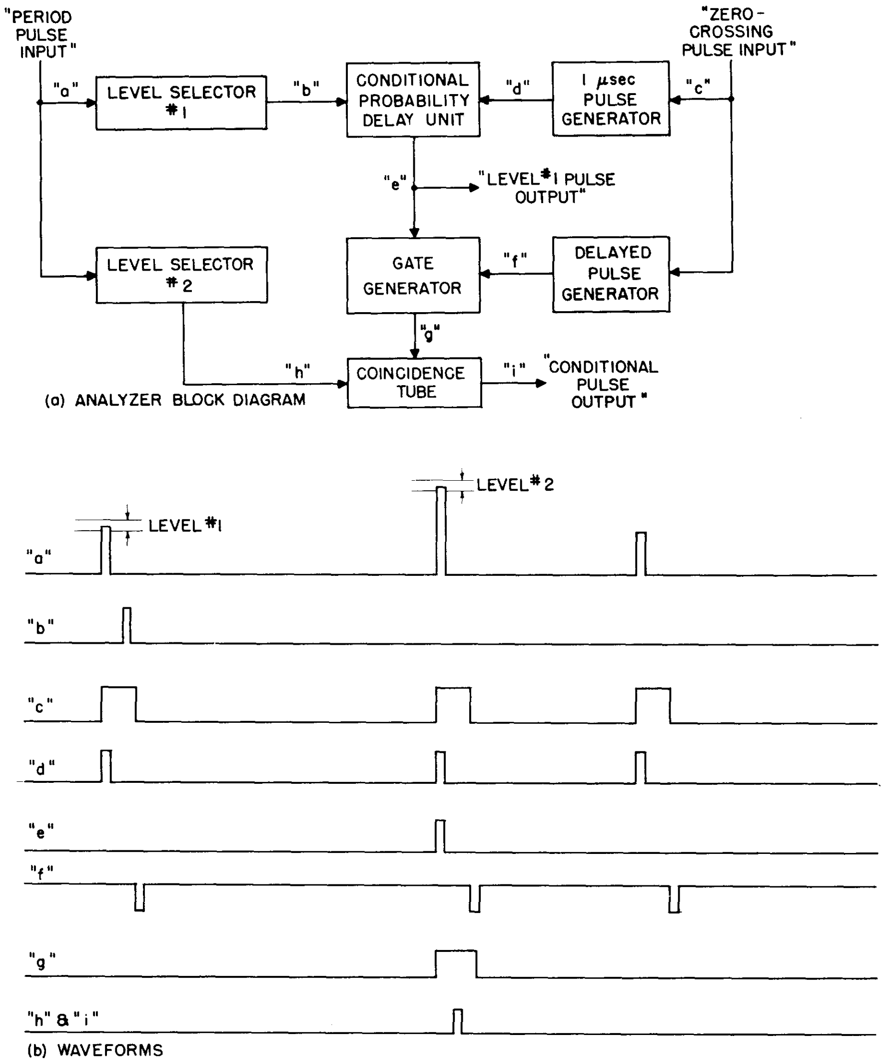

Fig.IX-13 (a) zero-crossing period, conditional probability distribution analyzer; (b) waveforms.

Certain of the pertinent waveforms in this analyzer are given in Figure IX-13(b). The case shown is for the study of the first period after the given period.

The method of operation is as follows: the inputs to the system are the varying amplitude-period pulses ("a") and the constant-amplitude zero-crossing pulses ("c"). These pulses are to be obtained from the zero-crossing probability analyzer discussed in the Progress Report of January 15, 1949. Whenever a period pulse lies within level #1, a pulse ("b") is generated to start the conditional-probability delay unit. Also applied to the delay unit are pulses ("d") corresponding to the zero-crossing times. As determined by the setting of the delay unit, a number of zero-crossings after the occurence of a period pulse in level #1, a pulse ("e") is obtained from the delay unit. This pulse ("e") is used to start a gate generator. The end of the gate pulse ("g") is determined by a delayed zero-crossing pulse ("f"). If, at this later time, a period pulse occurs in level #2, a pulse ("h") is obtained from the second-level selector. If such a pulse occurs, then coincidence with the gate waveform ("g") occurs, and an output pulse is generated.

The relative frequency of occurence of the period corresponding to level #2, n-periods after the occurence of a period corresponding to level #1, is then given by the ratio of the number of the conditional pulses ("i") obtained to the number of level #1 pulses ("e") used to determine coincidence.

Prof. R. M. Fano, W. B. Davenport, Jr.

3. Optimum Prediction

A predictor circuit based on Wiener's statistical theory of the design of linear transmission circuits has been completed. Following the procedure suggested in the last progress report, the predicted time function is narrow-band random noise. A block diagram of the predictor is shown in Figure IX-14.

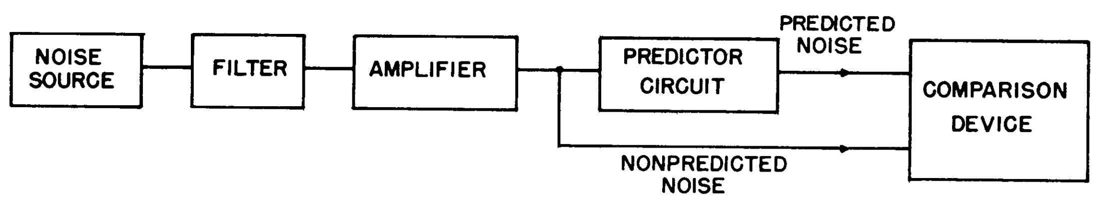

Fig. IX-14 Block diagram of predictor.

The noise source is a 6D4 gas triode which provides a substantially flat noise spectrum to well above 100 kc/sec. The filter is a simple tuned circuit having a resonant frequency of about 1000 cycles/sec and a Q variable in steps from 10 to 95. The predictor circuit has the following system function:

$$H(\omega) = e^{-\frac{\omega_o \alpha}{2Q}} \sin \omega_o \alpha \left[\cot \omega_o \alpha - \frac{1}{2Q_o} + \frac{1}{-j\frac{\omega}{\omega_o}} \right] ,$$

where ω_o is the resonant angular frequency of the tuned circuit and α is the prediction time. The design provides for three values of $\omega_o\alpha$ -- 22 1/2°, 45°, and 67 1/2°. The mean-square error in prediction, normalized with respect to the input noise power, is

$$\epsilon = \left[1 - e^{-\frac{\omega_o \alpha}{Q}} \right] .$$

Two means of comparing the predicted and nonpredicted noise are: (a) simultaneous display on a two-beam oscilloscope, and (b) cross-correlation (the position of the first peak in a cross-correlation indicates the prediction time). Both of these methods have indicated a close agreement between theory and practice. Pictures of the waveforms and correlation curves have not yet been prepared.

Prof. Y. W. Lee, C. A. Stutt

4. Pulse-Modulation Studies

A Technical Report entitled "Interference Characteristics of Pulse-Time Modulation" is in preparation. A paper on the same subject was presented at the National Convention of the Institute of Radio Engineers.

Prof. J. B. Wiesner, E. R. Kretzmer

5. Storage of Pulse-Coded Information

The major change which has been made in the storage system described in the last Progress Report is to use step, instead of linear, horizontal deflection on the storage tubes. The reason for the change is that the flexibility of the system is increased. The system in its present state will function with either periodic or nonperiodic pulses.

The required input will be the "write" trigger pulses (the binary signal pulses occuring simultaneously with the write trigger pulses), and the "read" trigger pulses. All of these pulses will probably have to be a fraction of a microsecond wide, and of several volts amplitude. The only limitations on the occurence of the write and read pulses are that the storage tube in which reading is taking place must be emptied before the tube in which writing is taking place is filled to capacity, and that the smallest time interval between adjacent pulses must be equal at least to a minimum value $\underline{d}$. The former limitation is due to the fact that only two storage tubes are used. The latter is primarily due to the writing and reading times of the storage tubes. Each of these times is about 5 microseconds at present; since the deflection circuits will require about 2 microseconds to move the electron beam of a tube to the next position, the value of $\underline{d}$ is about 7 microseconds.

The step-generator circuit which will be used in the deflection units has been designed and tested. It is shown in Figure IX-15. The current-source tubes are adjusted to draw 0.5, 1, 2, 4, and 8 milliamperes, and are turned on and off by the associated flip-flops. The voltage across the common load resistor consists of 32 equal-amplitude steps, from 0 to 15.5 volts. No noticeable difference in the step amplitudes is indicated by a precision milliammeter connected in series with the load resistor. The circuit has been operated, at a 100-kilocycle-per-second rate, for several days. The step amplitudes were checked periodically, and the maximum deviation from the correct values was less than 1 per cent; in most cases, the deviation was less than 0.5 per cent.

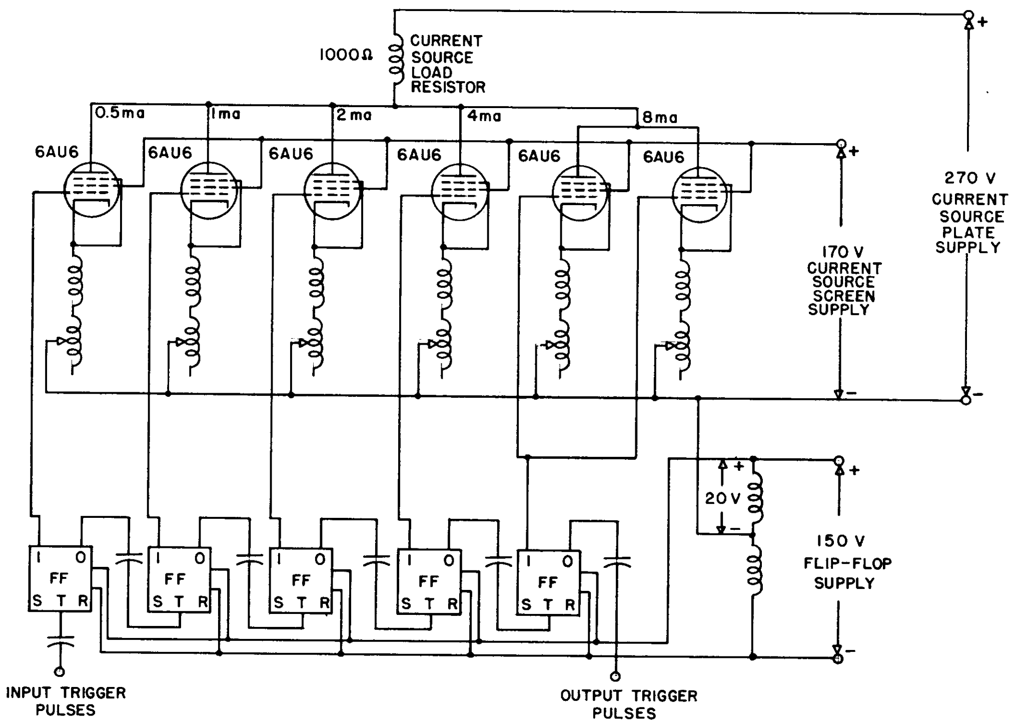

Fig. IX-15 Block schematic diagram of deflection-unit step generator. The potential of current-source grids with respect to the positive side of the flip-flop supply is 0 volts when side 1 of flip-flop is not conducting, -40 volts when side 1 is conducting.

A direct-coupled amplifier has been designed which will provide a balanced output of 250 volts maximum, peak-to-peak, with negligible deviation from linearity. The first stage is a cathode-coupled 6SN7 phase inverter. The use of a 6AK6 pentode, instead of a resistor, as the common cathode resistance results in a difference of about 1 per cent in the gains of the two halves of the 6SN7. A second 6SN7 supplies the additional required gain; the gains of its two halves can be adjusted to compensate for the difference in the gains of the first-stage tube. The output tube is a 5687 dual triode, operated as two cathode followers, which drives the unterminated line feeding the storage-tube deflection plates. The excellent linearity is obtained by using relatively large cathode resistances in each half of each 6SN7. Testing of the amplifier will be commenced shortly.

The final equipment will probably occupy two relay racks. The two storage tubes and their deflection units will be in one rack, and the control unit and power supplies in the other. Construction of this equipment will not be started until after the control unit, which routes the pulses and controls the operation taking place in each storage tube, has been designed.

Prof. J. B. Wiesner, A. J. Lephakis

6. "Felix" (Sensory Replacement)

This project has encountered numerous equipment troubles. Tests will start immediately when these are cleared up.

Prof. N. Wiener. Prof. J. B. Wiesner, E. E. David, Jr., L. Levine

a. Bank Filters With Variable Bandwidths

The present Felix equipment employs filters which break the audio spectrum into channels which are adjacent in their frequency ranges, but which are well defined and overlapping to only a negligible degree. The output from this device contains no indication of the location of a single tone within the channel range, but only the knowledge of the particular range in which the tone appears. Were the present filter network to be replaced by channels of a fairly wide and overlapping spread, more information about the position of the tone on the spectrum could be obtained by comparing the outputs of adjacent channels.

For this purpose, a bank of five filters with associated amplifiers is being built. Each filter channel will consist of an amplifier with a Twin T degenerative feedback circuit. Such a circuit is preferable to an RC-controlled stage as originally proposed. Ganged condensers will be used for constant control of center frequency. Control of the amount of feedback will provide continuous adjustment of the bandwidth.

Prof. R. M. Fano, E. M. Howlett, A. M. Lang

7. Low-Frequency Output Spectrum of Lock-In Amplifier

A Technical Report (No. 105) on the work of this project is in manuscript form and will be published shortly.

Prof. J. B. Wiesner, C. A. Stutt

8. Clipped-Speech Studies

A considerable amount of work on the intelligibility of clipped speech has been done at Harvard by Dr. J. C. R. Licklider and others. The aim of our study is to carry further this work by investigating the same problem from the point of view of information theory.

In particular, the short time-average rate of zero crossings of the wave will be determined as a function of time. From this, an attempt will be made to reconstruct the speech wave from the information remaining after the clipping and averaging operations. This phase of the investigation is a continuation of the work reported by D. F. Winter in the Quarterly Progress Report of October 15, 1948.

Subsequently, a comparison will be made of the auto-correlation function of the speech wave before and after clipping. Differentiation before clipping will be studied from the point of view of its effect on the auto-correlation function and the rate of zero crossings.

A speech clipper is being built with facilities for differentiating the speech wave, essentially as described by Dr. J. C. R. Licklider (2). A speech clipper utilizing a slicing circuit is also being built. This will permit a comparison of the two methods of clipping. A voltage proportioned to the rate of zero crossings will be obtained using a circuit similar to British Patent No. 562791 and to a scheme developed at the Bell Telephone Laboratories (3). In this scheme, the clipped wave is applied to a pulse-producing circuit which generates one pulse per zero crossing. These pulses are of uniform height and duration and are averaged to provide a measure of the rate of zero crossings.

Prof. R. M. Fano, P. E. A. Cowley

9. Pulse-Code Magnetic Recorder

Three different decoders -- one on a current-adding basis, two on a voltage-adding basis -- have been designed. Seven channels for each of the voltage-adding schemes and one channel of the current-adding scheme have been built. Partial tests have proved satisfactory but a final judgment and a relative evaluation of the different schemes can be made only after the playback amplifier and the recorded signal are available.

Since, in the absence of the recorded signal, the design of the amplifier is difficult, effort is now concentrated upon the design of a suitable driving mechanism and, further, upon the study of suitable recording, playback and erasing heads and the waveforms which can be expected off the tape. While the design of the entire amplifier is not yet finished, it has been decided to abandon the original idea of squaring the obtained playback waveform after equalization and to use only the steepest part of the equalized playback waveform to trigger a one-shot multivibrator whose output pulse length would be constant (e.g., 20 microseconds). In this arrangement having a peaker circuit (to trigger the multivibrator), a multivibrator has been designed and is being built at the present time.

Several filters of the Tchebychev type have been designed, built and tested experimentally; these are to be used later at the output of the decoder. The six-element low-pass filters were designed to have a constant response up to 10 kc, and as small a response as possible for the higher frequencies. A suitable unit was obtained. The greatest deviation from the constant value in the pass-band was about 1 db, and at 20 kc the response is down about 37 db.

Prof. J. B. Wiesner, L. Dolansky

D. TRANSIENT PROBLEMS

Prof. E. A. Guillemin W. H. Kautz
Dr. M. V. Cerrillo D. M. Powers

1. Transient Theories

In the syncopated theory of integration it can be shown (R. L. E. Technical Report No. 55) that transients can be classified into families or classes, in accordance with the analytic structure of the integrand. All transients of a given class are equivalent to a generalized one, when suitable and simple transformations are introduced. The generalized transient is expressed in terms of the so-called "generating function", which express intrinsic relations between the amplitude and the phase functions. Generating functions appear in the form of three-dimensional solids and a particular transient corresponds to a cross section, along a suitable trajectory, of these solids. Solutions for other problems, not necessarily transients, which lead to some integrals, are contained also in these generating solids.

The most important generating functions are expressed

a. In terms of functions of Lommel;

b. In terms of extended Airy-Hardy integrals;

c. In terms of Fresnell functions.

Although the last two can be expressed also in terms of Lommel functions, one keeps the above separation for practical reasons of their application and computation. Besides, the third is a subcase of the second. In general, the generating functions are functions of complex variables.

During the last three months, work has been directed towards the numerical computation of the generating functions. The initial steps for the

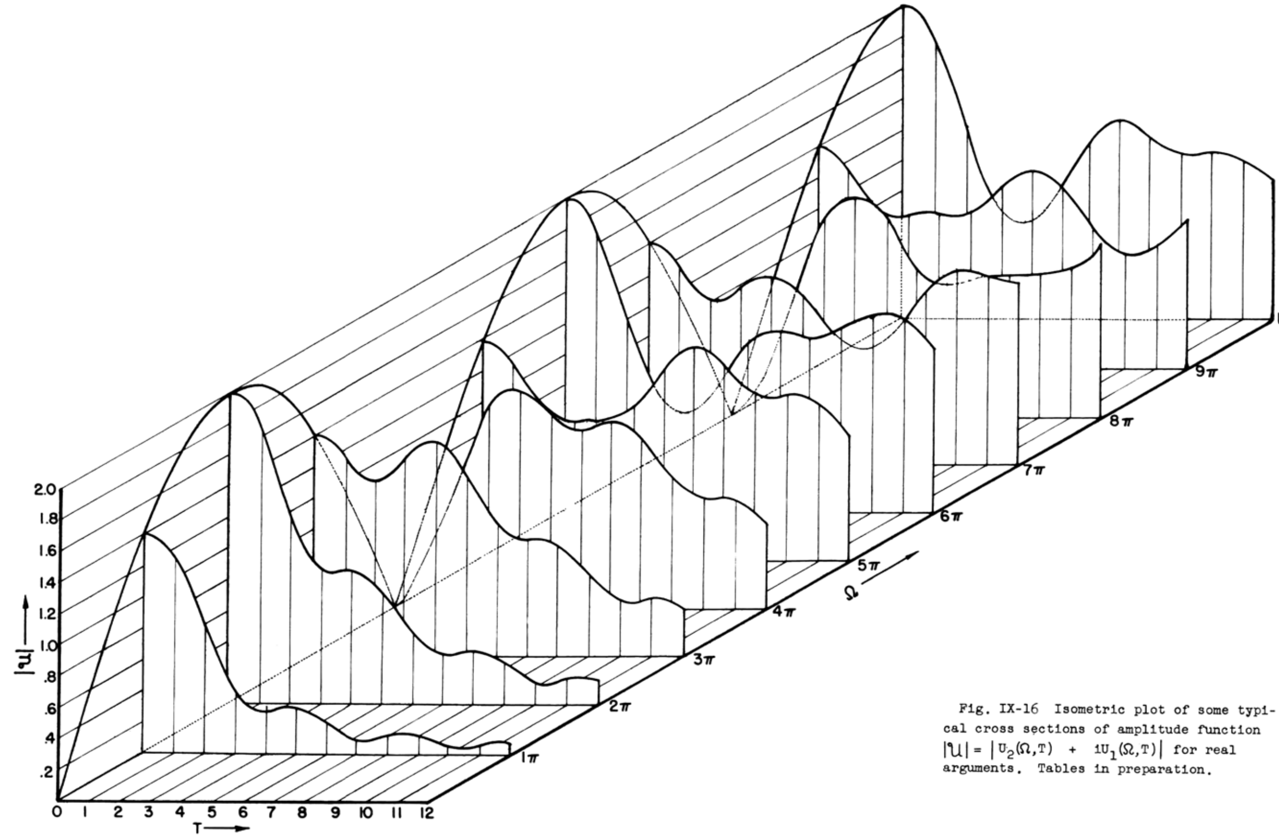

Fig. IX-16 Isometric plot of some typical cross sections of amplitude function $|\mathcal{U}| = |U_2(\Omega,T) + iU_1(\Omega,T)|$ for real arguments. Tables in preparation.

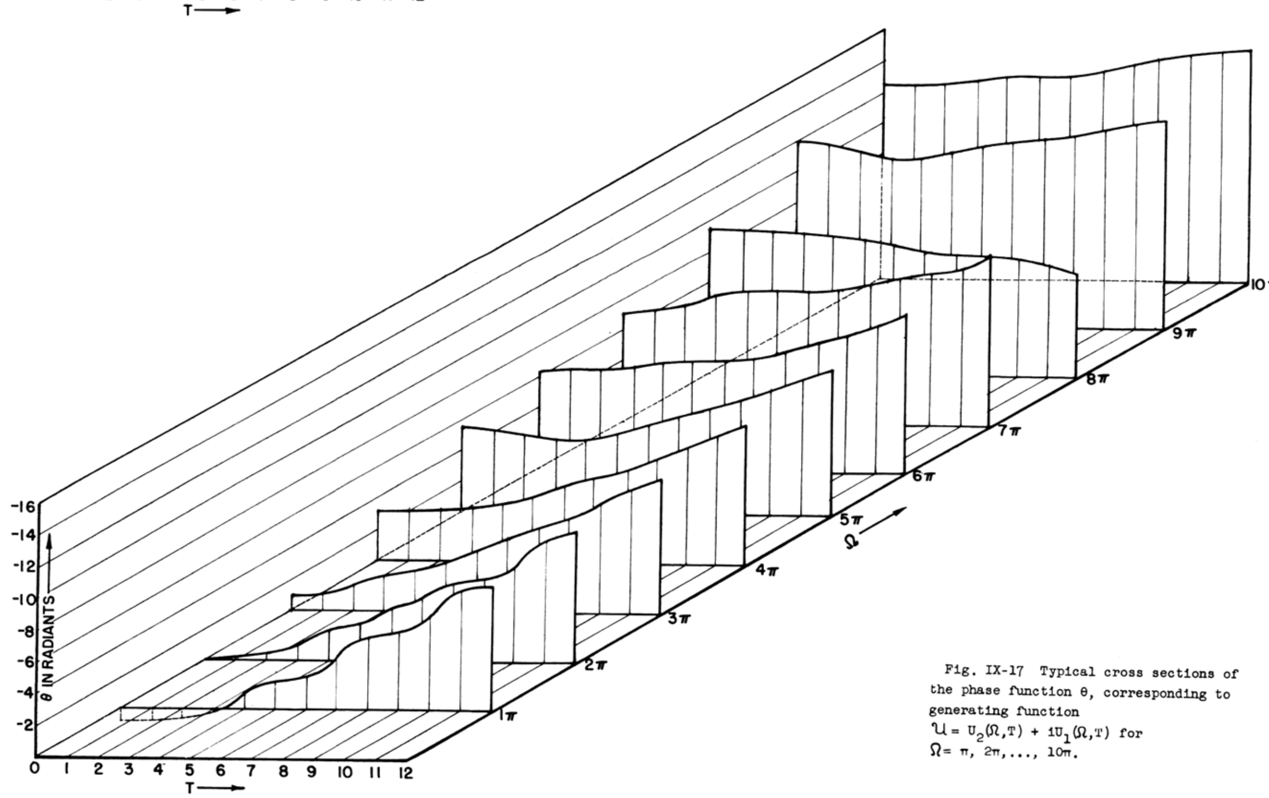

Fig. IX-17 Typical cross sections of the phase function θ, corresponding to generating function $\mathcal{U} = U_2(\Omega,T) + iU_1(\Omega,T)$ for $\Omega = \pi, 2\pi, \ldots, 10\pi$.

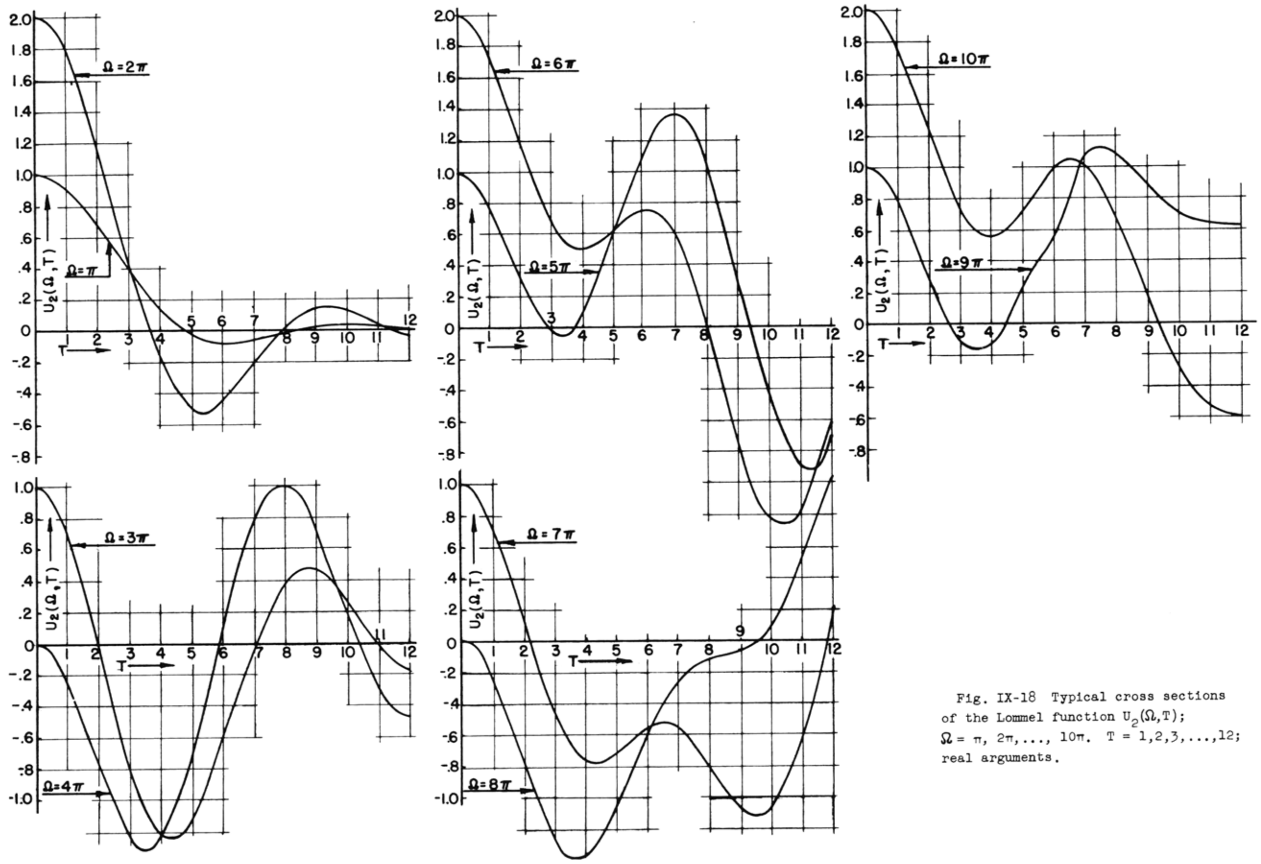

Fig. IX-18 Typical cross sections of the Lommel function $U_2(\Omega,T)$; $\Omega = \pi, 2\pi, \ldots, 10\pi$. $T = 1,2,3,\ldots,12$; real arguments.

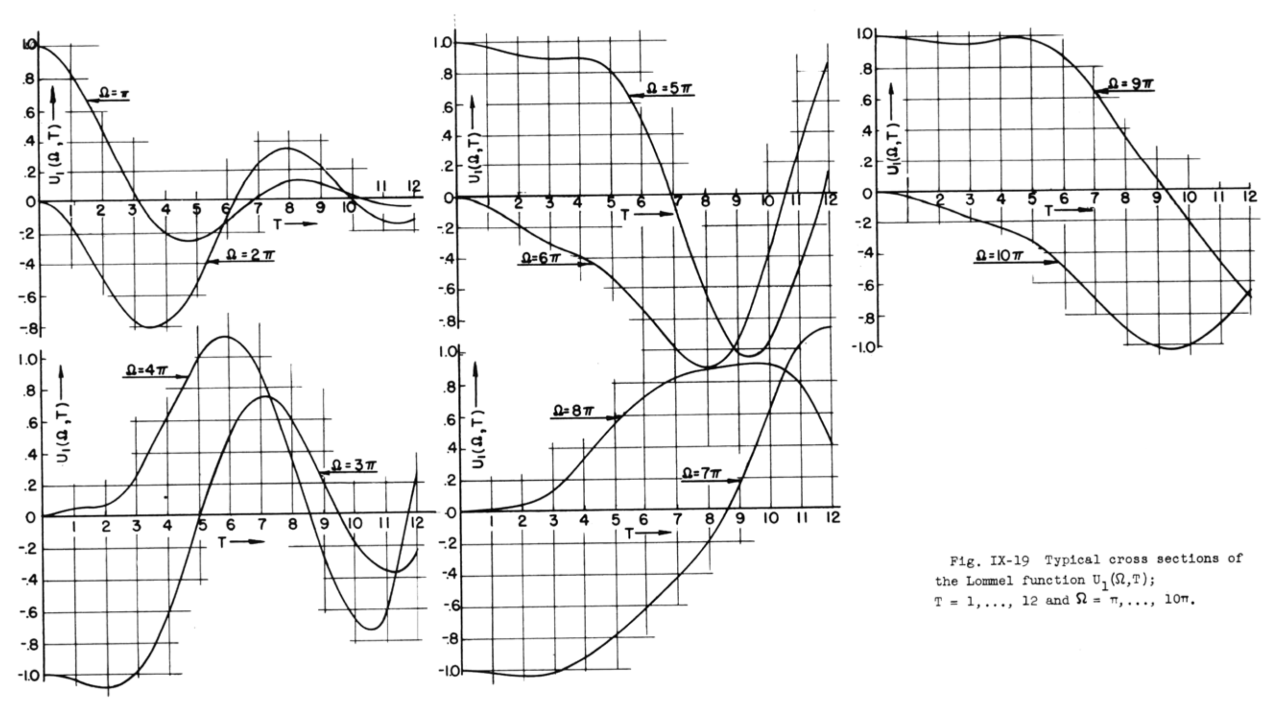

Fig. IX-19 Typical cross sections of the Lommel function $U_1(\Omega,T)$; $T = 1,\ldots, 12$ and $\Omega = \pi,\ldots, 10\pi$.

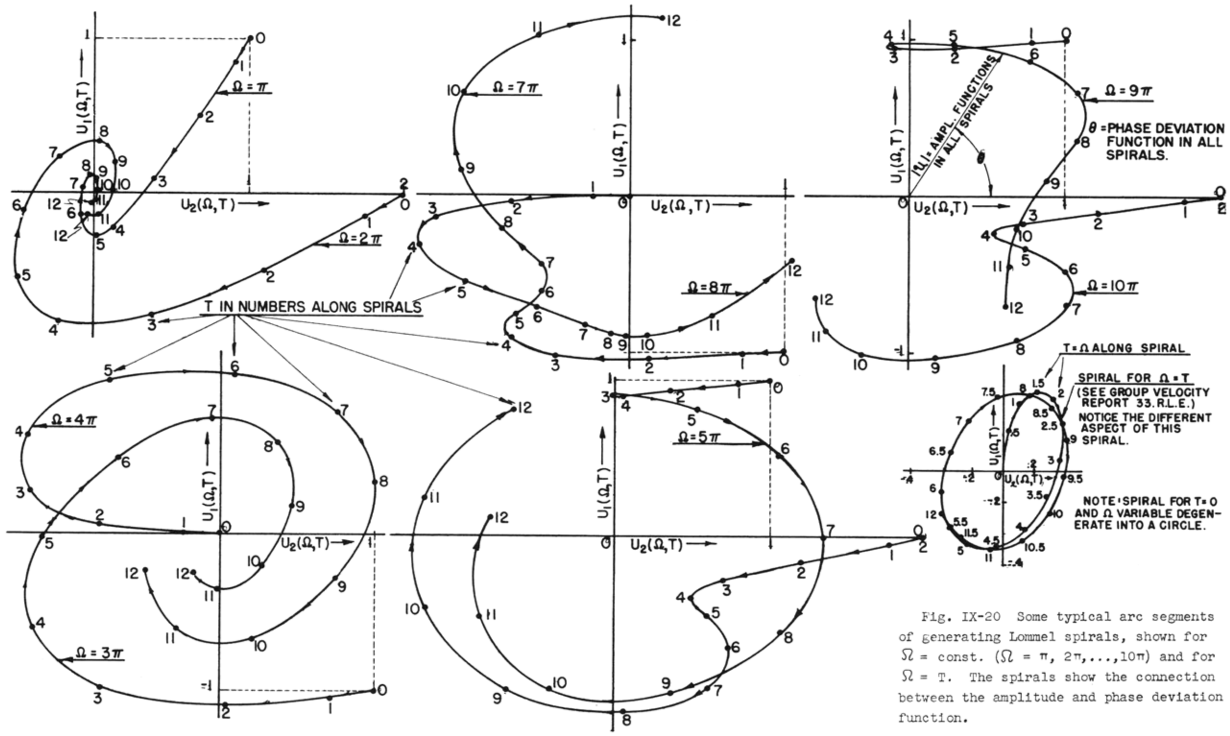

Fig. IX-20 Some typical arc segments of generating Lommel spirals, shown for Ω = const. ($\Omega = \pi, 2\pi, \ldots, 10\pi$) and for $\Omega = T$. The spirals show the connection between the amplitude and phase deviation function.

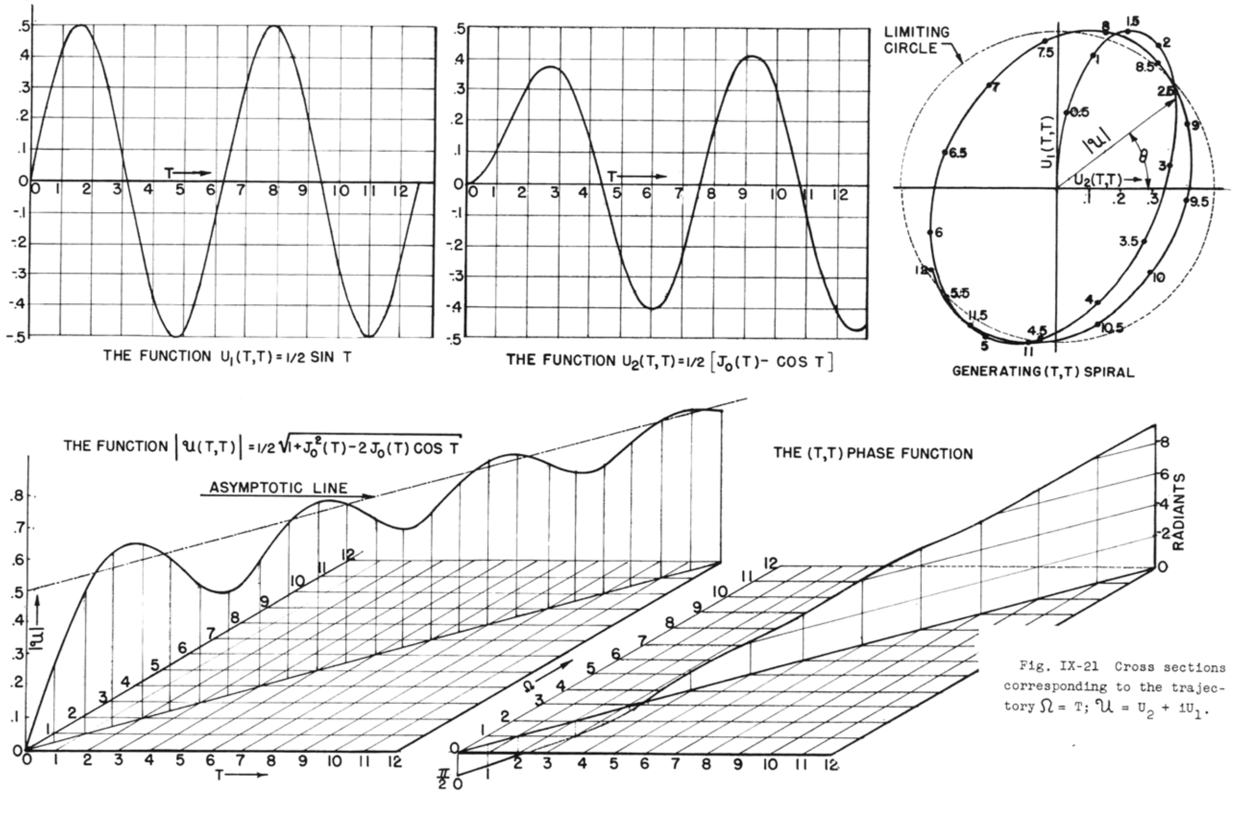

Fig. IX-21 Cross sections corresponding to the trajectory $\Omega = T$; $\mathfrak{U} = U_2 + iU_1$.

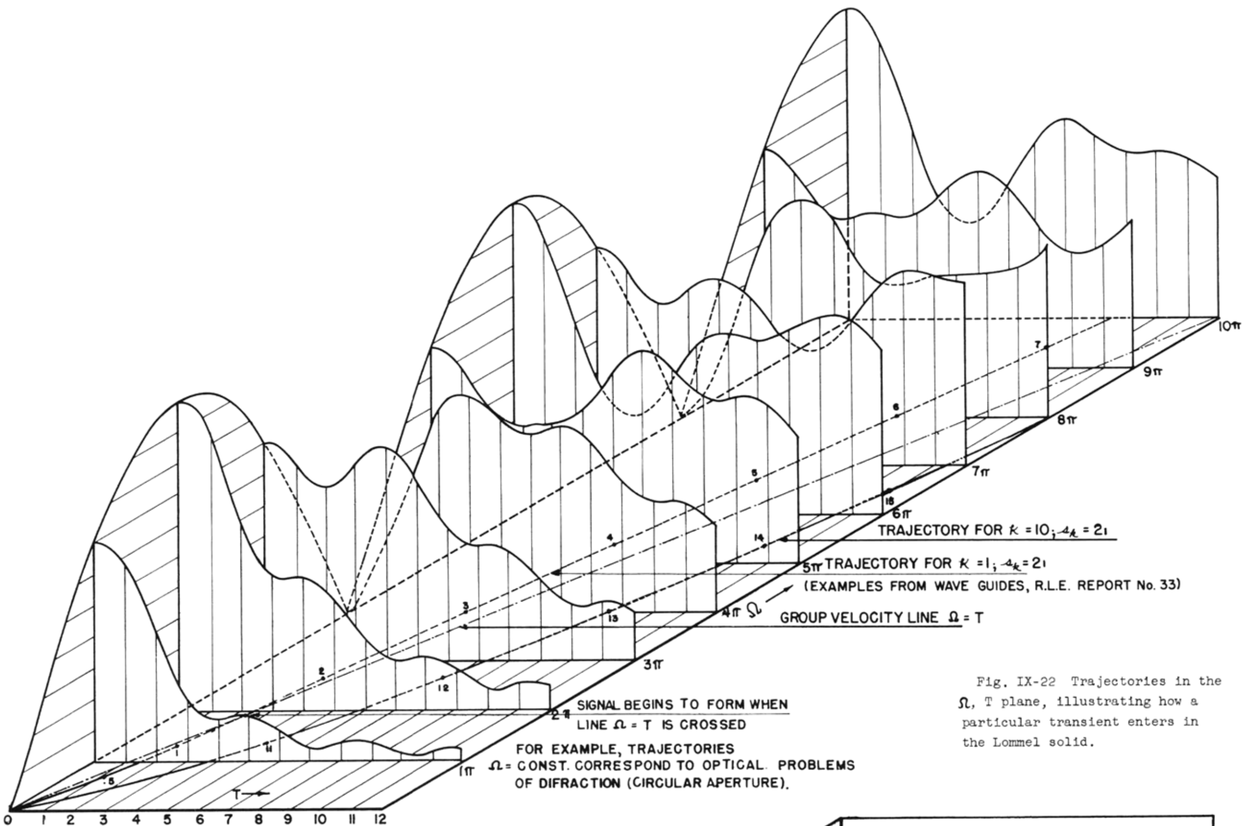

Fig. IX-22 Trajectories in the Ω, T plane, illustrating how a particular transient enters in the Lommel solid.

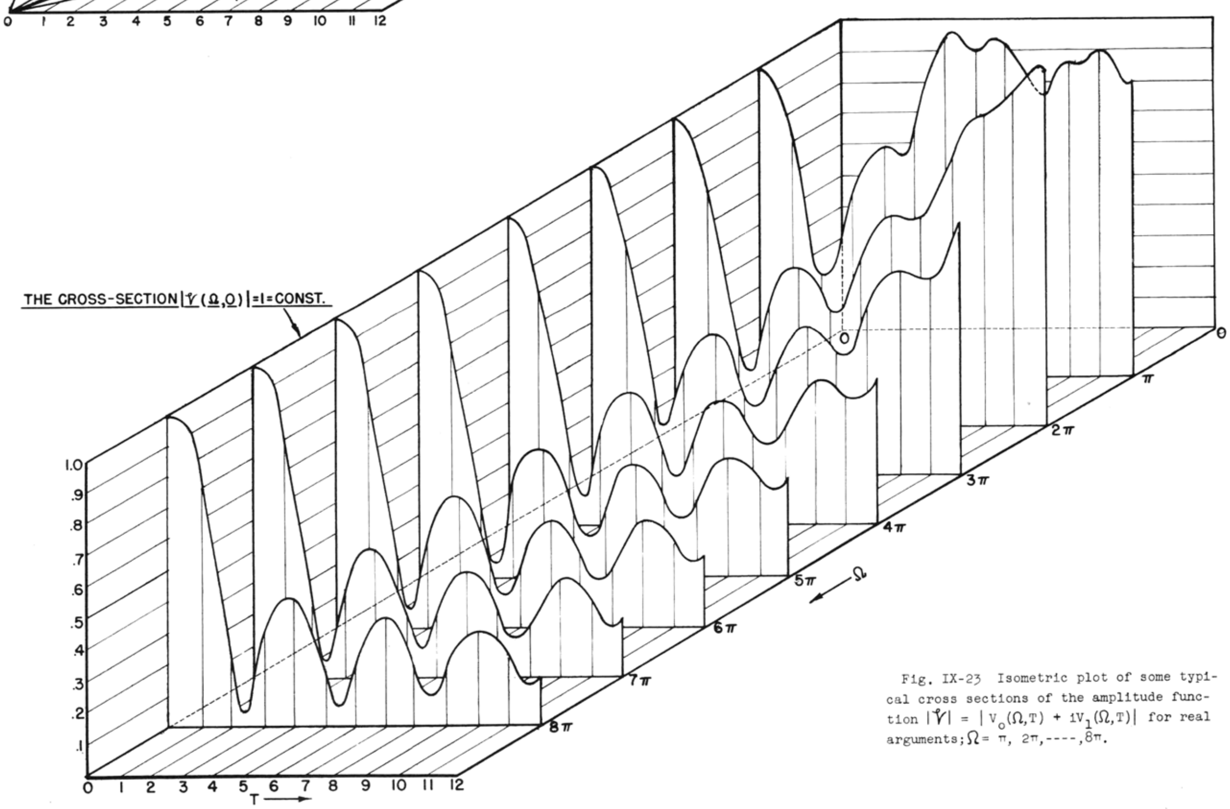

Fig. IX-23 Isometric plot of some typical cross sections of the amplitude function $|\mathcal{V}| = |V_0(\Omega,T) + iV_1(\Omega,T)|$ for real arguments; $\Omega = \pi, 2\pi, ----, 8\pi$.

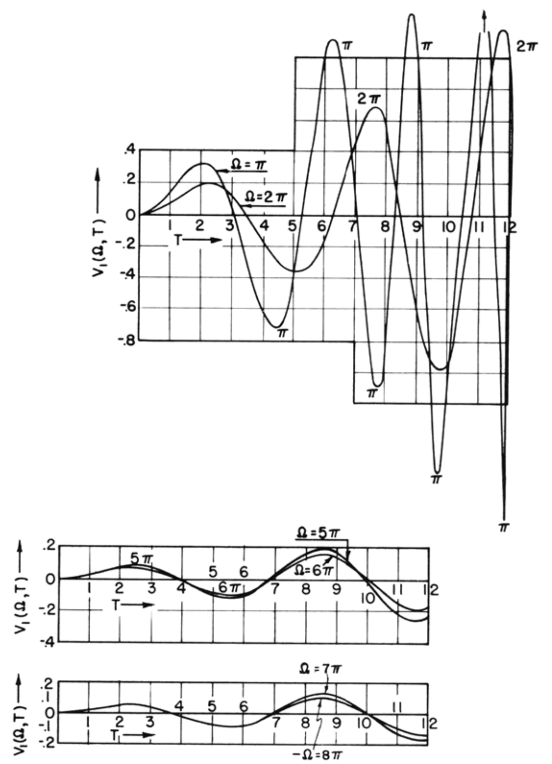

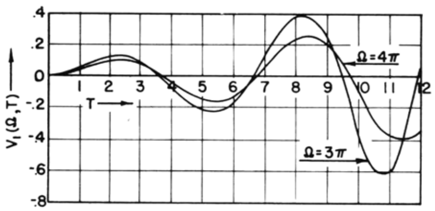

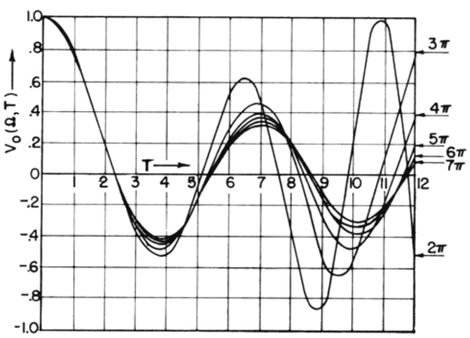

Fig. IX-24 Typical cross sections of the Lommel functions $V_0(\Omega, T)$ for real arguments; $\Omega = \pi, 2\pi, \ldots, 8\pi$.

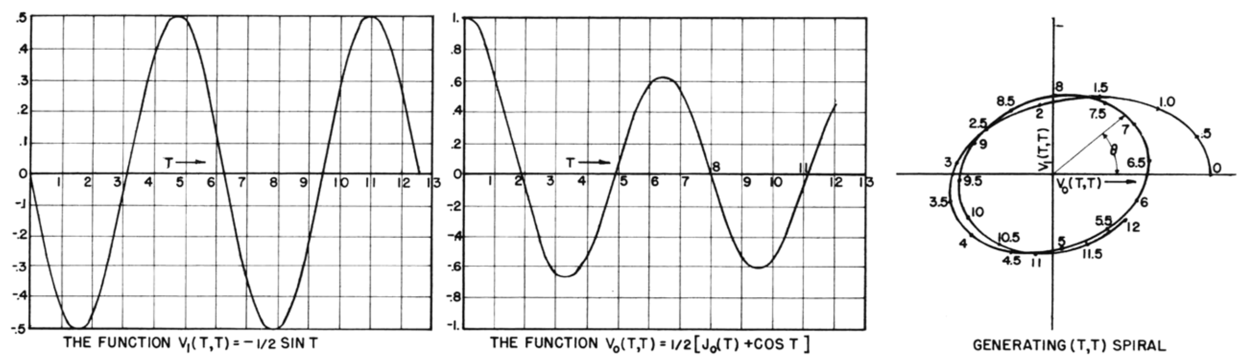

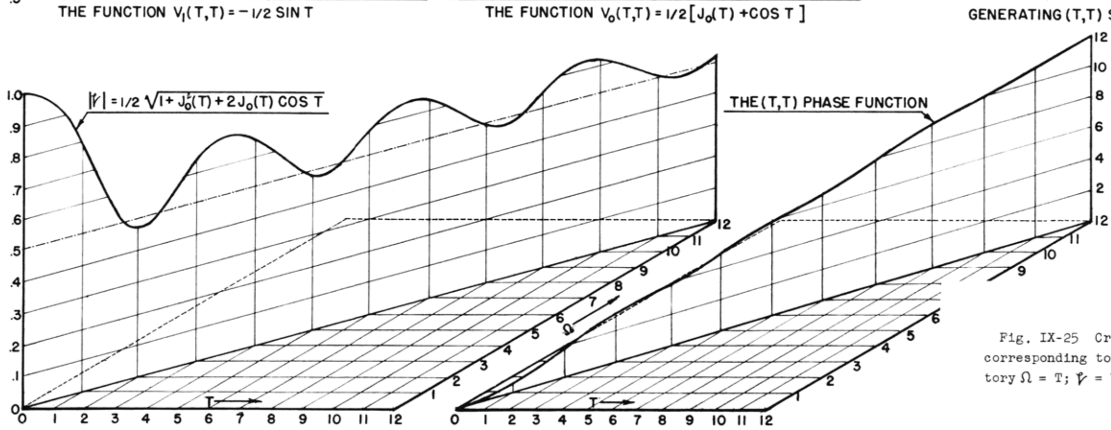

Fig. IX-25 Cross sections corresponding to the trajectory $\Omega = T$; $\gamma = V_0 + iV_1$.

computation have been started, mainly of the Lommel functions.

Lommel himself tabulates some of these functions. They cover the first two or three cycles of oscillation. He did not, in fact, compute his functions directly, but their products, with some variable factors needed in the applications in problems of the diffraction of light. His work appears in various sources (4)(5)(6). Lord Rayleigh (7) and Gray, Mathews and Robert (8) reproduce Lommel's tabulation exactly.

Conrady (9) and Buxton (10) give some figures of the light-intensity rings in stars, which, in a practical sense, does not render anything different from Lommel's original tabulation.

Here are presented, for the first time, some graphs of pure Lommel functions. They were obtained by a six-place direct computation from the Newmann series expansions and also by extracting them from the original Lommel tables. W. H. Kautz of this Laboratory is now computing Lommel functions corresponding to straight-line trajectories.

All this work represents the initial steps in preparing the numerical computations of the functions. Arrangements among R. L. E. Cambridge Field Stations (Drs. Spencer and Parke) and Harvard (Profs. Brillouin and Aiken) are under way to produce the tabulation of the Lommel functions.

Some work will be soon started in connection with the computation of the Airy-Hardy extended function. With regard to a complete tabulation of Fresnell's functions with complex argument, D. M. Power, of this Laboratory is now working in this connection with his studies of frequency-modulation transients.

Dr. M. V. Cerrillo

2. Theory of Synthesis of Networks for Specific Transient Response

Preparatory to the application of Dr. Cerrillo's transient theories to the solution of network synthesis problems, rough plots of the Lommel solids -- the generating functions for transients -- must be obtained. The preliminary results are shown in the accompanying figures.

Figure IX-26 illustrates the cross sections of the solid of the Lommel U-function corresponding to radial trajectories at various angles in the Ω - T plane. The trajectories corresponding to actual transients are curved arcs in this plane, and it may be seen from the solid that the largest changes in the amplitude (or envelope) of the transient occur when a trajectory crosses the 45° line ($\Omega/T = 1$). The instant of crossing is the line of "formation" of the transient, while the parts of the trajectory to either side of this line can contribute only to the precursor or to the

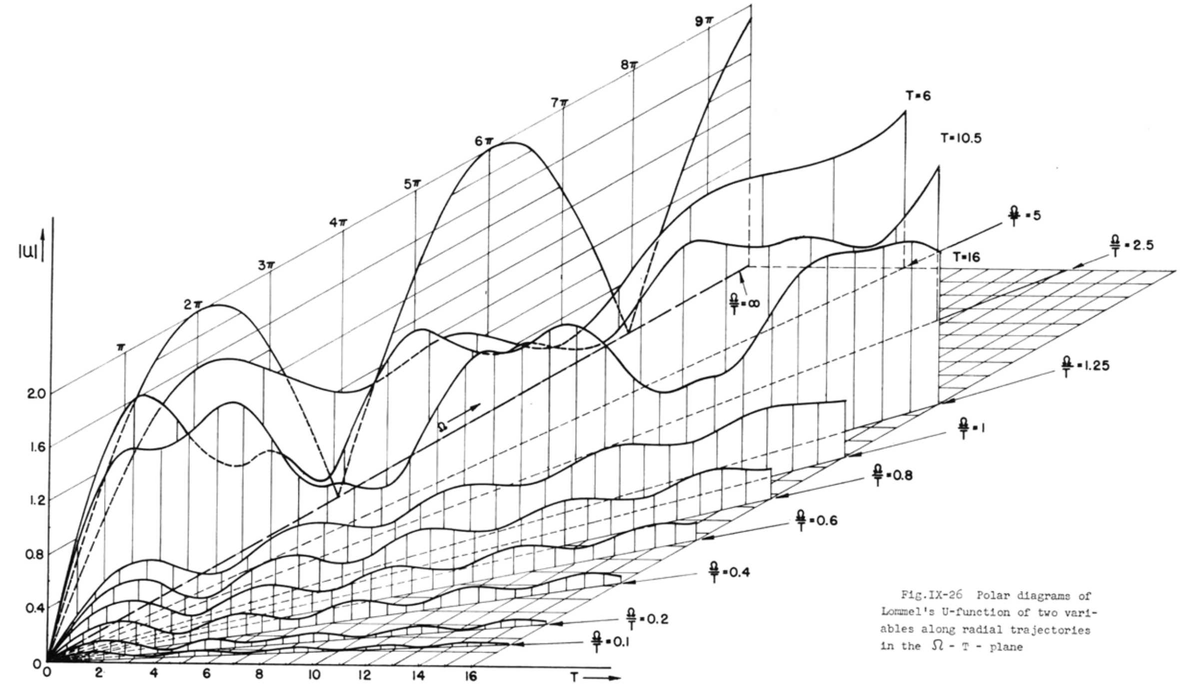

Fig.IX-26 Polar diagrams of Lommel's U-function of two variables along radial trajectories in the Ω - T - plane

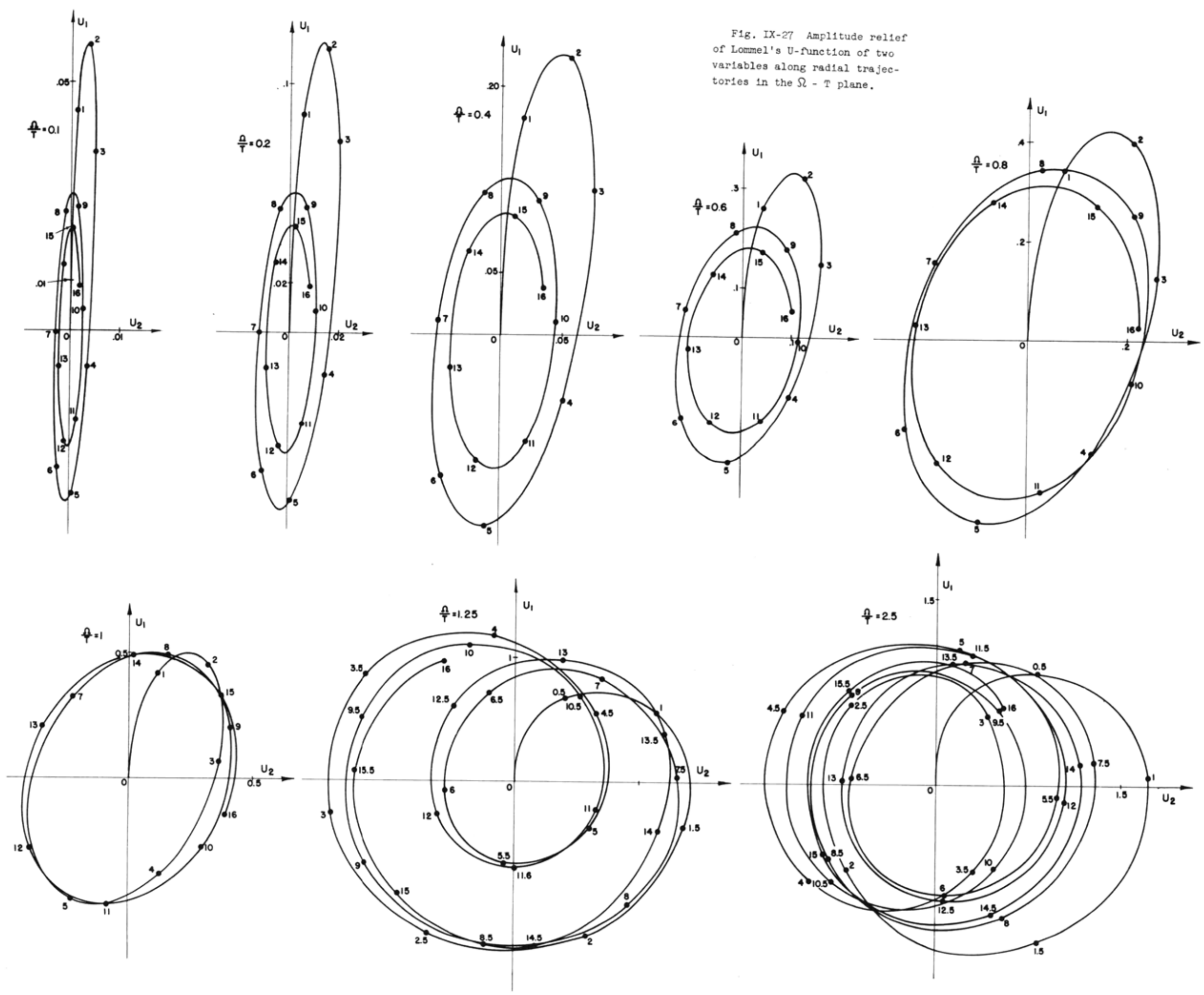

Fig. IX-27 Amplitude relief of Lommel's U-function of two variables along radial trajectories in the Ω - T plane.

coda parts of the wave. The variables Ω and T are functions of the time and, in the case of networks, of the positions of the poles and zero of the stimulus and network in the complex frequency plane.

Figure IX-27 shows the polar plots of the Lommel U-functions along these radial trajectories. Here

$$\mathcal{U} = U_2 + jU_1 = |U| e^{i\theta} \quad .$$

If some part of the transient is generated by passing along any of these lines, the situation may be visualized with the aid of a vector extending from the origin to a moving point on the spiral. As t (hence, T) increases, the length of this vector, measuring the amplitude of the transient, increases, but may oscillate very erratically. The increasing angle which the vector sweeps out represents relative phase. It is conceivable that if some or all of the poles and zeros of a network yielding this transient may be chosen at will, the choice might be made so that the resulting trajectory yields a transient of some desired variety. The individual sections of the wave may be influenced relatively independently of one another, since they are generated by different trajectories in the Lommel solid.

The other three solids of interest -- that of the phase function θ associated with U, those of the amplitude and phase of the Lommel θ-function -- are being computed and plotted, and will appear in a subsequent progress report.

M. H. Kautz

3. Response of Networks to Frequency Transients

The function

$$\frac{1}{2} + \frac{1}{\sqrt{\pi}} \int_0^z e^{-it^2} dt$$

has been computed. This function is an important generating function in the solution of transient-response problems, particularly in the case of a linear frequency sweep applied to a pair of conjugate poles. A report on this subject is being prepared.

Prof. E. A. Guillemin, D. M. Powers

E. ACTIVE NETWORKS

Prof. E. A. Guillemin
Dr. M. V. Cerrillo J. G. Linvill

1. Broadband Amplifiers with Active Interstages

As discussed in previous progress reports, the method considered for obtaining amplifiers with arbitrary gain-bandwidth product was the use of active interstages. As described in those reports, the interstages consist of a passive part and an active part. The active part is a chain of cascaded conventional amplifiers fed by the tube supplying the interstage. The chain of amplifiers feeds current back into the passive part of the interstage which includes the inevitable parasitic capacitance. The basic idea is that the current from the chain of amplifiers could supply the parasitic capacitance and compensate for the limitation it imposes. The chain of amplifiers constituting the active part must still have appropriate parasitic capacitance associated with each stage. In the design of such an active interstage, several involved and interrelated conditions must be met. The impedance of the interstage must be large and approximately constant over the prescribed band. (Its level determines the gain of the amplifier.) The reciprocal of the interstage impedance must be split between the active and passive parts of the interstage, which are essentially in parallel. The component of admittance associated with the passive part must be a positive real function and the component associated with the active part must be identifiable with the amplification function of a chain of conventional amplifiers which have parasitic capacitances in each stage. The parasitic capacitance in each of the stages imposes a limit on the level of impedance of the active interstage, but no general way was discovered to evaluate the limit. Neither was a general practical method discovered for choosing the functions (the impedance of the active interstage, the amplification function of the chain of amplifiers, and the positive real impedance of the passive part).

It became apparent in the study of the problem that some of the techniques for designing chains of amplifiers, which were being applied with little success to the design of an active interstage, could be successfully applied to the design of wide-band amplifiers of another type. Accordingly, attention was shifted to this different possibility. The type of amplifier successfully treated consists of paralleled chains of conventional amplifiers in which each chain amplifies a suitably chosen narrow band of frequencies. The outputs of the chains are paralleled at the load. By controlling the magnitude of amplification and phase shift of the individual chains in a systematic manner, one can obtain an amplifier in which an arbitrary band of frequencies is amplified with approximately uniform magnitude and linear phase shift. The features of the method are the flexibility with which the frequency characteristics are controlled and the economy in the number tubes required for a specified gain and bandwidth. The accompanying Figure IX-28 shows the equivalent circuit of one example.

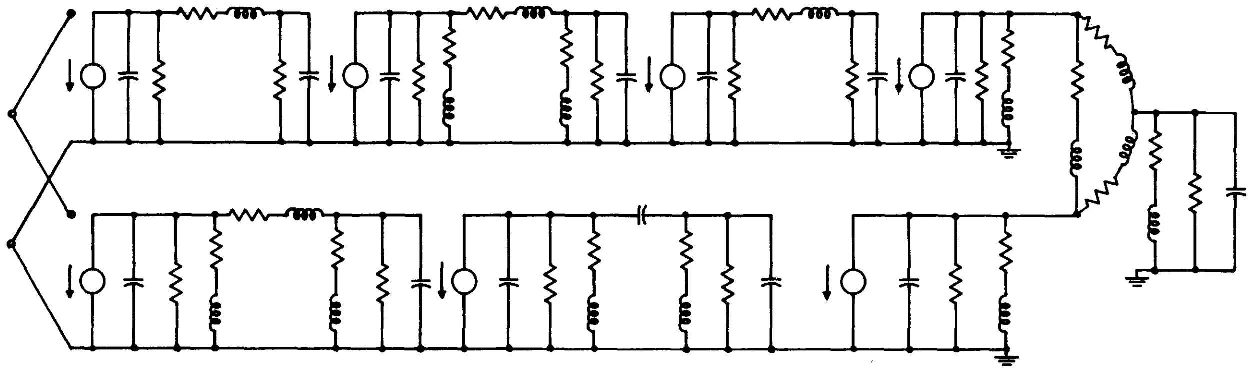

CALCULATED AMPLIFICATION 32 USING 7 6AK5 TUBES

Fig. IX-28 Equivalent circuit of 100-megacycle amplifier.

At present, the thesis based on this problem is being written. Subsequently, two technical reports will be prepared. The first will cover the solution of the approximation problem used for the amplifier problem. The approximation problem arises whenever one needs to specify suitable rational functions identifiable with a driving point or transfer function of a network (here, the amplification of a chain of amplifiers). The problem is to specify a realizable function with approximately the required magnitude and phase variation with frequency. The same method applied here to amplification functions could be applied in a wide range of problems in network theory. The second report will cover the amplifier problem, describing the design procedure and implemented by the approximation technique covered in the first report.

Prof. E. A. Guillemin, J. G. Linvill

F. HIGHER MODE PROBLEMS

Prof. L. J. Chu

R. B. Adler T. Moreno

1. Steady-State Propagation of Electromagnetic Waves Along Cylindrical Structures

Because the manuscript for a report (No. 102) on the subject is now in preparation, no further details of progress on this problem will be given here.

Prof. L. J. Chu, R. B. Adler

2. Techniques for Millimeter-Wave Transmission

A doctoral thesis ("On Transmission Techniques Suitable for Millimeter Waves") has been completed, and a technical report on the subject is forthcoming shortly.

Prof. L. J. Chu, T. Moreno

G. LOCKING PHENOMENA IN MICROWAVE OSCILLATORS

Prof. J. B. Wiesner
E. E. David, Jr.

The manuscript of Technical Report No. 100 is being completed and will summarize results obtained since Technical Report No. 63 was published. Experimental and theoretical work is continuing.

References

(1) M. Kulp, Spektra und Klirrfaktoren frequenz- und amplitudenmodulierter Schwingungen, El. Nachr. Tech. 19, 96 (1942).
(2) J. C. R. Licklider, J. Acous. Soc. Am. 20, No. 1, 42 (1948).
(3) "The Technical Aspects of Visible Speech", Bell Telephone System Monograph B-1415.
(4) "Bayerische Akademie der Wissenschaften" Munchen Abhandlungen 15, 229 (1885).
(5) Ibid., 15, 529 (1886).
(6) Ibid., 19, 449 (1899) (Pastume).
(7) Sci. Papers 3, 429 (1902).
(8) "Bessel Functions" (1899) (1922).
(9) Royal Astr. Soc. Monthly Notice 79, 575 (1919).
(10) Royal Astr. Soc. Monthly Notice 81, 547 (1921).

***